# Resonance Raman Spectroscopic Evidence for the $FeS_4$ and Fe–O–Fe Sites in Rubrerythrin from *Desulfovibrio vulgaris*[†]

Bakul C. Dave,[‡] Roman S. Czernuszewicz,[*,‡] Benet C. Prickril,[§] and Donald M. Kurtz, Jr.[§]

*Department of Chemistry, University of Houston, Houston, Texas 77204, and Department of Chemistry and Center for Metalloenzyme Studies, University of Georgia, Athens, Georgia 30602*

*Received November 4, 1993; Revised Manuscript Received January 18, 1994*[®]

ABSTRACT: Resonance Raman (RR) spectra of the non-heme iron protein rubrerythrin from *Desulfovibrio vulgaris* unequivocally demonstrate the presence of both a rubredoxin-type $FeS_4$ site and a ($\mu$-oxo)diiron(III) cluster. The RR spectra of rubrerythrin excited at 496.5 and 568.2 nm are dominated by bands similar to those of rubredoxin and conform to the vibrational pattern expected for a distorted $FeS_4$ tetrahedron of an Fe(S-Cys)$_4$ site. Numerous overtone and combination bands of the Fe–S stretches are also observed, and a band at 650 $cm^{-1}$ is assigned to a cysteine C–S stretching mode. The 374-, 355-, and 340-$cm^{-1}$ bands, assigned to the three components of the $\nu_3(T_2)$ asymmetric $FeS_4$ stretching mode, are 2–8 $cm^{-1}$ lower than the corresponding frequencies for the *Desulfovibrio gigas* rubredoxin $FeS_4$ site. Similar differences in frequencies of bands assigned to SFeS bending modes between rubredoxin and rubrerythrin are also detected. These frequency differences imply either slightly weaker Fe–S bonds or subtle conformational differences among the cysteinyl ligands in the rubrerythrin versus rubredoxin $FeS_4$ sites. The RR spectrum of rubrerythrin excited at 406.7 nm shows dramatically diminished intensities of the $FeS_4$ bands with concomitant enhancement of a band at 514 $cm^{-1}$. This band shifts 18 $cm^{-1}$ to lower frequency when the protein is dissolved in $H_2{}^{18}O$. The frequency of this band and the $^{18}O$ isotope shift are those expected for the symmetric Fe–O–Fe stretch of a bent oxo-bridged diiron(III) cluster and indicate that this cluster has at least one additional bridging ligand. A small but reproducible 2-$cm^{-1}$ shift to higher frequency of this symmetric Fe–O–Fe stretch in $D_2O$ may indicate involvement of the oxo bridge in hydrogen bonding.

Rubredoxin (Rd)[1] is a small iron–sulfur protein found in several anaerobic bacteria. While Rd is believed to function as an electron transfer agent, the biological role of Rd in most organisms is ill-defined. On the other hand, Rd is a structurally well-characterized protein containing a single pseudotetrahedral Fe(S-Cys)$_4$ site (Day et al., 1993, and references therein). ($\mu$-Oxo/hydroxo)diiron sites are found in a diverse group of proteins, such as hemerythrin and ribonucleotide reductase, in which the diiron site usually (though not always) interacts with $O_2$ during the functional process (Wilkins, 1992). Recently, a novel protein given the trivial name "rubrerythrin" was discovered (LeGall et al., 1988), whose spectroscopic properties strongly suggest the presence of both Rd-type $FeS_4$ sites and a ($\mu$-oxo/hydroxo)diiron cluster. Rubrerythrin has been isolated from the anaerobic sulfate-reducing bacterium *Desulfovibrio vulgaris* (Hildenborough). The as-isolated protein was reported to consist of a homodimer (subunit $M_r$ 21 900) and to contain four iron atoms arranged as two Rd-type $FeS_4$ sites and one antiferromagnetically coupled diiron cluster. More recent experiments (Ravi et al., 1993) show that rubrerythrin can be reconstituted such that each subunit contains a diiron cluster as well as an $FeS_4$ site and, together with amino acid sequence comparisons (Kurtz & Prickril, 1991), suggest that the oxidized form of the diiron cluster bears a close structural (but not necessarily functional) resemblance to that of the ($\mu$-oxo)($\mu$-carboxylato)diiron(III) cluster in oxidized ribonucleotide reductase. The crystals of rubrerythrin have been examined by X-ray crystallography at 3.0- (Sieker et al., 1988) and 2.3-Å (Stenkamp et al., 1992) resolutions and four cysteine ligands near the Rd-like center and four glutamate and two histidine ligands analogous to those binding irons in ribonucleotide reductase near the diiron center have been identified, but no structures of the metal clusters are available. The biological function of this unique combination of prosthetic groups in rubrerythrin remains to be established. The visible absorption, EPR, and Mössbauer spectra of the $FeS_4$ site in rubrerythrin are quite similar to those of Rd in both oxidized and reduced forms of the proteins. However, the midpoint reduction potential of the $FeS_4$ site in rubrerythrin (~+230 mV) is about 250 mV more positive than that of Rd (LeGall et al., 1988; Pierik, 1993). Mössbauer spectra of both the as-isolated and reconstituted rubrerythrin show that the oxidized diiron cluster consists of an antiferromagnetically coupled pair of five- or six-coordinate high-spin ferric irons with oxygen and/or nitrogen ligands.

We have sought additional probes to confirm and extend these previous structural conclusions about the $FeS_4$ sites and diiron clusters in rubrerythrin. Resonance Raman (RR) spectroscopy has been shown to be a particular insightful structural probe of both $FeS_4$ sites in oxidized Rd ($Rd_{ox}$) (Spiro et al., 1988) and of ($\mu$-oxo)diiron(III) sites in hemerythrin and ribonucleotide reductase (Sanders-Loehr, 1989). S →Fe or $\mu$-O →Fe charge-transfer (CT) electronic transitions are found in the visible or near-UV regions, respectively, for $Rd_{ox}$

---

[†] This work was supported by National Institute of General Medical Sciences–NIH Grant GM-48370 (to R.S.C.), by Robert A. Welch Foundation Grant E-1184 (to R.S.C), and by National Institutes of Health Grant GM40388 (to D.M.K.). D.M.K. is an NIH Research Career Development Awardee 1988–1993 (HL02207).

[*] To whom correspondence should be addressed.

[‡] University of Houston.

[§] University of Georgia.

[®] Abstract published in *Advance ACS Abstracts*, March 1, 1994.

[1] Abbreviations: Rd, rubredoxin; $Rd_{ox}$, oxidized rubredoxin; RR, resonance Raman; EPR, electron paramgnetic resonance; CT, charge transfer; HB(pz)$_3$, hydrotris(1-pyrazolyl)borate; tacn, 1,4,7-triazacyclononane; hdp, *N*-(*o*-hydroxybenzyl)-*N*,*N*-bis(2-pyridylmethyl)amine; tpa, tris(2-pyridylmethyl)amine; phen, 1,10-phenanthroline; hedta, *N*-(hydroxyethylethylene)diaminetriacetate; OAc, acetate; OBz, benzoate.

0006-2960/94/0433-3572$04.50/0

or the diiron proteins. With laser excitations tuned to these CT transitions, Fe–S or Fe–O–Fe stretching vibrational modes can be preferentially enhanced in RR spectra of the respective proteins. Since analogous S →Fe and $\mu$-O →Fe CT transitions are apparently observed for rubrerythrin (LeGall et al., 1988), this protein is an attractive target for RR studies. In this work we examine the RR spectra of *D. vulgaris* rubrerythrin in $H_2O$, $H_2{}^{18}O$, $D_2O$, and $D_2{}^{18}O$ at cryogenic temperatures using variable wavelength excitation to extract the vibrational signatures of the $FeS_4$ and diiron sites and to resolve the question of the bridging ligand in the latter cluster.

## MATERIALS AND METHODS

*Protein Purification and Isotopic Substitution.* The growth of *D. vulgaris* (Hildenborough) and the purification of rubrerythrin were performed as previously described (LeGall et al., 1988). The as-isolated protein in 0.1 M Tris-HCl, pH 7.6, was stored at -20 °C. $D_2O$ (99.9% D) and $H_2{}^{18}O$ (98% $^{18}O$) and $D_2{}^{18}O$ (99% D, 98% $^{18}O$) were obtained from Isotec (Miamisburg, OH) and Cambridge Isotopes, Inc. (Woburn, MA), respectively. The as-isolated rubrerythrin was crystallized by spontaneous crystallization upon protein concentration. The crystalline protein was then redissolved in 30 $\mu$L of $H_2{}^{18}O$, $D_2O$, or $D_2{}^{18}O$ to an approximate concentration of 1 mM directly in a gold-plated copper cup of a Raman liquid-$N_2$ Dewar (see below). The isotopically substituted samples were allowed to equilibrate for 10–15 min before freezing.

*Resonance Raman Spectroscopy.* RR spectra were obtained using lines from Coherent K-2 $Kr^+$ (406.7, 530.9, and 568.2 nm) and 90–6 $Ar^+$ (496.5 nm) ion lasers by collecting front-scattering directly from the surface of a frozen protein solution held in vacuo on a liquid $N_2$-cooled cold finger. Under these conditions no protein damage was observed, even during prolonged (6–12 h) spectral data acquisition at laser powers of 200–400 mW. Details of this sampling technique are presented elsewhere (Czernuszewicz & Johnson, 1983). To ensure accurate isotopic measurements, the protein samples in four waters ($H_2O$, $D_2O$, $H_2{}^{18}O$, and $D_2{}^{18}O$) were placed side by side on the gold-plated copper cold finger so that the RR data could be collected under the same conditions. Conventional scanning Raman instrumentation equipped with a Spex 1403 double monochromator and a Hamamatsu 928 photomultiplier detection system was used to record the spectra under the control of a Spex DM3000 microcomputer system (Czernuszewicz, 1993). The spectral slit width was 6 cm$^{-1}$ and the spectrometer was advanced in 1-cm$^{-1}$ increments over the range 100–1700 cm$^{-1}$ for the initial survey spectra (not shown) and in 0.5-cm$^{-1}$ increments over smaller ranges for detailed spectra (Figures 1–3). Integration times were 1 s per point for all spectra. Multiple scans (5–7) were averaged to improve signal-to-noise ratios. Slowly sloping baselines were subtracted out of the digitally collected spectra by using LabCalc software (Galactic Industries Corporation) mounted on a 486-DX 33 MHz PC microcomputer. All spectra were calibrated using the known vibrational modes of $CCl_4$ and $CH_2Cl_2$. A Hewlett-Packard 8-pen ColorPro graphics plotter was used for hard copy output spectra.

## RESULTS AND DISCUSSION

Figure 1 shows low-temperature (77 K) RR spectra of as-isolated *D. vulgaris* rubrerythrin in a liquid $N_2$ cell with excitation at 496.5 and 406.7 nm. These excitation wavelengths should be in resonance with the 492- and 368-nm absorption bands, respectively, of rubrerythrin (LeGall et al., 1988). Figure 2 compares RR spectra obtained with 406.7-nm excitation for the protein contained in $H_2O$ and the recrystallized protein dissolved in $H_2{}^{18}O$, $D_2O$, and $D_2{}^{18}O$. The dashed lines correlate shifted bands due to the same vibrational modes. Figure 3 shows 450–550-cm$^{-1}$ RR spectra with 406.7- (upper two) and 496.5-nm (lower two) excitations, in $H_2O$ and $H_2{}^{18}O$, which serves to demonstrate how a combination of the wavelength-dependent RR selectivity and isotopic substitution helps to resolve overlapping band structure in this region. Band frequencies, isotope shifts, and assignments are listed in Tables 1 and 2. Also listed for comparison purposes are low-temperature RR data previously reported for $Rd_{ox}$ from *D. gigas* (Table 1) and for diiron(III) forms of hemerythrin, ribonucleotide reductase, and synthetic oxo-bridged complexes (Table 2).

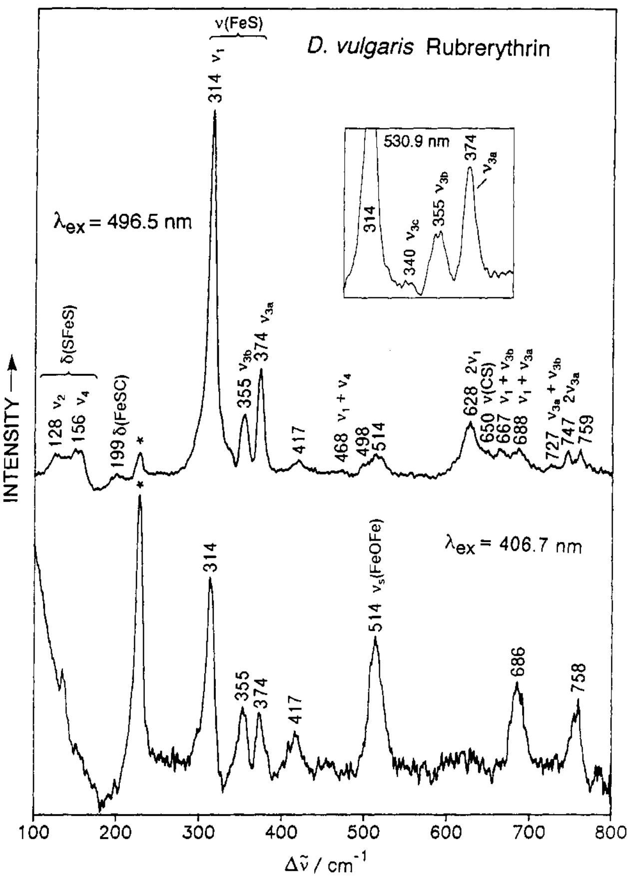

FIGURE 1: Low-temperature (77 K) RR spectra of as-isolated *D. vulgaris* rubrerythrin obtained in the 100–800-cm$^{-1}$ region with 496.5- (upper trace) and 406.7-nm (lower trace) excitation wavelengths. the inset shows details of the $\nu_3$ Fe–S stretching region excited at 530.9 nm. Conditions: front-scattering from the surface of a frozen protein solution kept in a liquid-$N_2$ Dewar; 150 mW of laser power; 6-cm$^{-1}$ slit widths; average of six scans, with each scan having a 1-s integration time at 0.5-cm$^{-1}$ increments. Asterisks indicate the 228-cm$^{-1}$ ice band.

*$FeS_4$ Sites.* The Fe(S-Cys)$_4$ site of oxidized rubredoxins has a distinctive series of four Fe–S stretching vibrations between 310 and 380 cm$^{-1}$ involving mostly symmetric and asymmetric changes in the four iron–cysteine bond lengths (Spiro et al., 1988). The 496.5-nm excited RR spectrum in Figure 1 is overwhelmingly dominated by the vibrational modes characteristic of $Rd_{ox}$-type $FeS_4$ sites. The number, positions, and intensities of these resonance enhanced Raman bands closely match those observed for frozen solutions of $Rd_{ox}$ from *Desulfovibrio gigas* (Table 1) (Czernuszewicz et al., 1986). Since 496.5-nm excitation is in resonance with the S →Fe CT electronic transition, whose effect is to weaken the Fe–S bonds in the excited state, the spectrum is further dominated by the

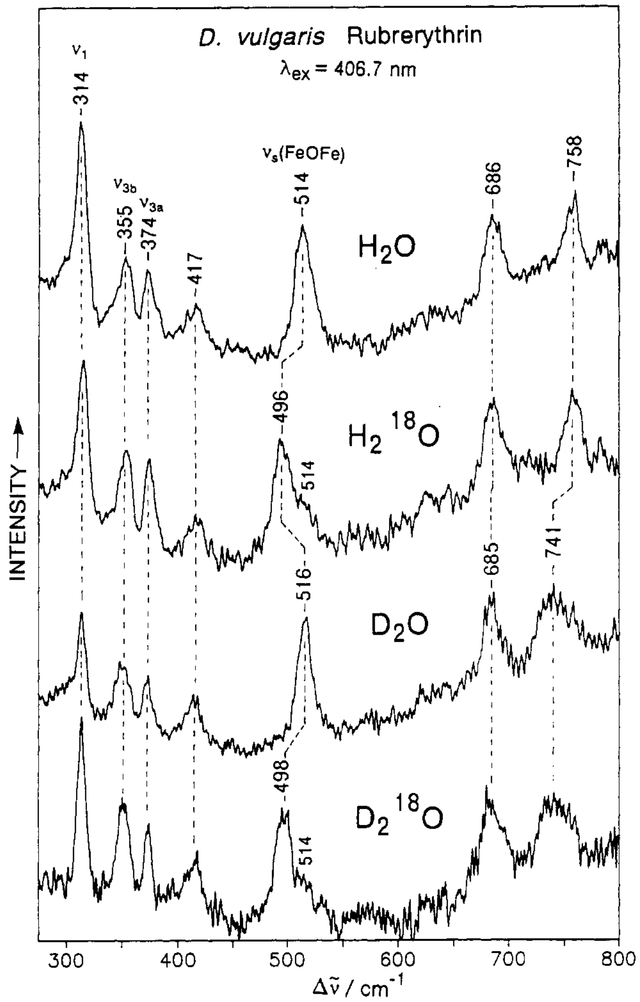

FIGURE 2: 406.7-nm excited RR spectra (300–800 $cm^{-1}$) of *D. vulgaris* rubrerythrin (77 K) contained in $H_2O$, $H_2{}^{18}O$, $D_2O$, and $D_2{}^{18}O$, showing the effects of $^{16/18}O$ and H/D exchange on the resonance-enhanced vibrational modes. Conditions are as in Figure 1.

Fe–S stretching bands. The most intense of these bands at 314 $cm^{-1}$ matches exactly the frequency of the polarized band observed for *D. gigas* $Rd_{ox}$ and is very close to the corresponding band at 312 $cm^{-1}$ observed for $Rd_{ox}$ from several other sources (Yachandra et al., 1983). This band is assigned to the totally symmetric breathing mode of the $FeS_4$ tetrahedron, $\nu_1$ ($A_1$ in idealized $T_d$ symmetry). The first overtone of this mode can also be detected, $2\nu_1$ at 628 $cm^{-1}$. In the 350-$cm^{-1}$ region, where the triply-degenerate asymmetric Fe–S stretch, $\nu_3(T_2)$, is expected, two bands are clearly detected, $\nu_{3a}$ at 374 $cm^{-1}$ and $\nu_{3b}$ at 355 $cm^{-1}$ (Figure 1). In addition, with 530.9- and 568.2-nm excitations, a third band appeared weakly in this region, $\nu_{3c}$, at 340 $cm^{-1}$ (Figure 1, inset). The assignment of these bands as components of the asymmetric Fe–S stretch is consistent with the assignment of peaks observed at 376 ($\nu_{3a}$), 363 ($\nu_{3b}$), and 348 ($\nu_{3c}$) $cm^{-1}$, which shift to higher frequency upon $^{54}Fe$ substitution into *D. gigas* $Rd_{ox}$ (Czernuszewicz et al., 1986). This assignment is further substantiated by a recent detailed analysis of the $FeS_4$ vibrational spectra of Rd model complexes.[2]

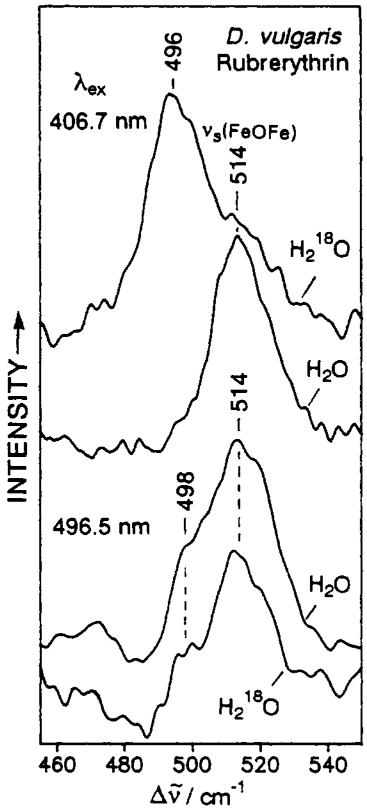

FIGURE 3: 460–540-$cm^{-1}$ RR spectra of *D. vulgaris* rubrerythrin (77 K) excited at 406.7 (upper two traces) and 496.5 nm (lower two traces), in $H_2O$ and $H_2{}^{18}O$, showing that by selective tuning of the laser excitation wavelengths and isotopic substitution it is possible to resolve overlapping bands arising from the Fe–O–Fe (514 $cm^{-1}$) and $FeS_4$ (498, 514 $cm^{-1}$) sites of rubrerythrin. Conditions are as in Figure 1, except that these spectra are smoothed.

Previous RR studies on $Rd_{ox}$ have shown the intense $\nu_1$ Fe–S band to be broad and asymmetric, implying more than one component to this band; e.g., for *D. gigas* $Rd_{ox}$ a clearly visible shoulder on the $\nu_1$ 314-$cm^{-1}$ band has been located at 324 $cm^{-1}$ in the high-resolution spectrum at 77 K and assigned to a S–C–C bending mode, $\delta$(SCC), on the basis of its insensitivity to isotopic substitution with $^{54}Fe$ (Table 1). We saw no indication of such a peak in the RR spectra of rubrerythrin. However, the frequency and intensity of the $\delta$(SCC) band can be quite variable, as demonstrated by the dramatically different shapes of the $\nu_1$ bands ($\sim$312 $cm^{-1}$) in the room-temperature RR spectra of $Rd_{ox}$ from several organisms (Yachandra et al., 1983) and the results of normal coordinate analysis calculations.[2]

Inasmuch as the $\nu_3$ Fe–S stretch splits into three components in the RR spectrum of rubrerythrin, the actual symmetry of its $FeS_4$ sites must be significantly lower than $T_d$, a situation which has been found for all Rds studied by RR spectroscopy. Normal coordinate analysis shows that the extent of splitting of the $\nu_3$ mode depends mainly on the magnitudes of the S–Fe–S angles and on the kinematic coupling between $\nu$(FeS) and $\delta$(SCC), which is greatly dependent on the Fe–S–C–C dihedral angles. Also, for a given set of the Fe–S–C–C dihedral angles, the frequency of $\nu_1$ is calculated to be about twice as sensitive to kinematic coupling as that of $\nu_3$ (Yachandra et al., 1983). Thus, even though the $\nu_1$ mode for rubrerythrin occurs at the same frequency as those of *D. gigas* $Rd_{ox}$, the 2–8 $cm^{-1}$ lower $\nu_{3a\text{-}c}$ Fe–S frequencies for rubrerythrin versus $Rd_{ox}$ imply some structural differences between the respective $FeS_4$ sites, such as slightly weaker Fe–S bonds in rubrerythrin and/or different cysteine conformations in the two proteins. The $\nu_2(E)$ and $\nu_4(T_2)$ S–Fe–S bending modes of rubrerythrin are located at 128 and 156 $cm^{-1}$, respectively, which are 2 $cm^{-1}$ lower and 6 $cm^{-1}$ higher than for *D. gigas* $Rd_{ox}$, further supporting subtle

---

[2] Czernuszewicz, R. S., Kilpatrick, L., Koch, S., & Spiro, T. G. (1994) *J. Am. Chem. Soc.* (submitted).

Table 1: Resonance Raman Frequencies ($cm^{-1}$) and Assignments for *D. gigas* Rubredoxin and *D. vulgaris* Rubrerythrin[a]

| *D. gigas* rubredoxin | *D. vulgaris* rubrerythrin | assignment |
|---|---|---|
| 130 | 128 | $\delta$(SFeS),[b] $\nu_2$,[c] $A_1(E)$[d] |
| 150 | 156 | $\delta$(SFeS), $\nu_4$, $E(T_2)$ |
| 174 |  | $\delta$(FeSC) |
| 184 | 199 | $\delta$(FeSC) |
| 314 | 314 | $\nu$(FeS), $\nu_1$, $A_1$ |
| 324 |  | $\delta$(SCC) |
| 348 | 340 | $\nu$(FeS), $\nu_{3c}$, $E(T_2)$ |
| 363 | 355 | $\nu$(FeS), $\nu_{3b}$, $E(T_2)$ |
| 376 | 374 | $\nu$(FeS), $\nu_{3a}$, $B_2(T_2)$ |
| 403 | 417 | ? |
| 443 | 442 | $\nu_1 + \nu_2$ |
| 463 | 468 | $\nu_1 + \nu_4$ |
| 502 | 498 | ? |
| 518 | 514 | ? |
|  | 514(−18)[+2][e] | $\nu_s$(FeOFe)[f] |
| 627 | 628 | $2\nu_1$ |
| 653 | 650 | $\nu$(CS) |
|  | 667 | $\nu_1 + \nu_{3b}$ |
|  | 686[−1] | ? |
| 689 | 688 | $\nu_1 + \nu_{3a}$ |
| 733 | 727 | $\nu_{3a} + \nu_{3b}$ |
| 751 | 747 | $2\nu_{3a}$ |
|  | 758[−17] | ? |
| 757 | 759 | $2\nu_1 + \nu_2$ |
| 777 |  | $2\nu_1 + \nu_4$ |

[a] Rubredoxin data and assignments from Czernuszewicz et al. (1986). Rubrerythrin data from this work. [b] $\delta_{xyz}$ and $\nu_{xy}$ are bending and stretching coordinates involving the indicated atoms. [c] $\nu_{1-4}$ are normal modes of a $XY_4$ tetrahedron. [d] Symmetry designation for the $D_{2d}(T_d)$ point groups. [e] The numbers in () and [] indicate the frequency shifts in $H_2{}^{18}O$ and $D_2O$, respectively. [f] $\nu_s$ is the symmetric (in-phase) Fe–O–Fe stretching coordinate.

structural differences between the Fe–S sites in these proteins. It is unclear whether such subtle alterations in the rubrerythrin $FeS_4$ site could contribute to its relatively high reduction potential (LeGall et al., 1988).

Finally, it can be seen in Figure 1 that overtone and combination bands associated with the $FeS_4$ fundamentals of rubrerythrin show appreciable intensity, as expected for RR scattering. One weak band in this region at ~650 $cm^{-1}$ does not correspond to a combination band and is assigned to the cysteine C–S stretching mode, in analogy to the assignment of the 653-$cm^{-1}$ band of *D. gigas* $Rd_{ox}$ (Table 1). There are also five Raman bands above 400 $cm^{-1}$ that have not been assigned; however, three of these bands at 417, 498, and 514 $cm^{-1}$ [the 514-$cm^{-1}$ peak is coincidently degenerate with the $\nu_s$(Fe–O–Fe) stretch; see Figure 3] clearly correspond to a similar set of bands observed previously in the RR spectra of *D. gigas* $Rd_{ox}$ at 403, 502, and 518 $cm^{-1}$, respectively (Czernuszewicz et al., 1986). The origin of these features, and of the other two $H_2{}^{18}O$-insensitive bands seen with 406.7-nm excitation at 686 and 758 $cm^{-1}$ (685 and 741 $cm^{-1}$ in deuterated waters, Figure 2), remains to be investigated.

*Diiron(III) Cluster.* The bent Fe–O–Fe moiety of ($\mu$-oxo)diiron(III) clusters has two vibrational stretching modes: an in-phase symmetric stretch, $\nu_s$(Fe–O–Fe), and an out-of-phase asymmetric stretch, $\nu_{as}$(Fe–O–Fe). Both of these modes have been observed in resonance Raman spectra of ($\mu$-oxo)diiron(III) proteins and synthetic models (Sanders-Loehr, 1989; Sanders-Loehr et al., 1989; Gómez-Romero et al., 1989; Norman et al., 1990; Turowski et al., 1990), and both are sensitive to $^{18}O$ substitution, especially when the Fe–O–Fe angle deviates appreciably from 180°. The $\nu_s$(Fe–O–Fe) band, observed between 395 and 540 $cm^{-1}$, is usually more intense than the $\nu_{as}$(Fe–O–Fe) band, observed between 750 and 840 $cm^{-1}$. As mentioned earlier, these bands are most strongly enhanced using near-UV excitation. The 406.7-nm excited RR spectrum of rubrerythrin (Figures 2 and 3) shows a peak at 514 $cm^{-1}$ which shifts to 496 $cm^{-1}$ upon $H_2{}^{18}O$ exchange. Therefore, the 514-$cm^{-1}$ band must involve vibrational motion of a water-exchangeable oxygen atom. This isotope shift is observed shortly after dissolving crystals of rubrerythrin in $H_2{}^{18}O$ (see Methods and Materials), which demonstrates that total incorporation of solvent oxygen in the vibrating ligand occurs very readily. Similarly facile oxo bridge exchange with solvent water is observed for ribonucleotide reductase, but not for methemerythrin (Sanders-Loehr, 1989). This observation is consistent with the structural similarity of the rubrerythrin diiron site to that of ribonucleotide reductase which was inferred from the amino acid sequence comparisons (Kurtz & Prickril, 1991) and suggests that the rubrerythrin diiron site is distinct from that of methemerythrin. When the rubrerythrin crystals are dissolved in $D_2O$, the 514-$cm^{-1}$ peak shifts 2 $cm^{-1}$ to higher frequency. The same 2-$cm^{-1}$ upward shift is observed in $D_2{}^{18}O$ versus $H_2{}^{18}O$ (Figure 2); thus, this small deuterium isotope shift appears to be reproducible. These frequencies and isotope shifts, when compared to those of other diiron(III) proteins and synthetic models (Table 2), allow assignment of the 514-$cm^{-1}$ peak to $\nu_s$(Fe–O–Fe) in rubrerythrin. Small upward shifts of $\nu_s$(Fe–O–Fe) in $D_2O$ for oxyhemerythrin and ribonucleotide reductase apparently indicate hydrogen bonding to the oxo bridge, and such hydrogen bonding is, thus, also indicated in rubrerythrin.

From the observed $\nu_s$(Fe–O–Fe) frequency (514 $cm^{-1}$) and its $^{18}O$ isotope shift (−18 $cm^{-1}$), an Fe–O–Fe angle of 124° can be calculated for the diiron cluster in rubrerythrin by solving a simple X–Y–X three-body vibrational problem (Wing & Callahan, 1969). This calculated angle is similar to those observed by X-ray crystallography of oxo-bridged diiron(III) clusters in proteins and synthetic models (Table 2). The rubrerythrin $\nu_s$(Fe–O–Fe) frequency and the magnitude of its $^{18}O$ shift are inconsistent with a monobridged Fe–O–Fe cluster (cf. Table 2), but are consistent with either a di- or tribridged cluster in which the additional bridging ligands are bidentate carboxylates. The present data are insufficient to distinguish between the latter two types, which so far represent the only ones known to occur in ($\mu$-oxo)diiron proteins (Holmes & Stenkamp, 1991; Holmes et al., 1991; Nordlund & Eklund, 1993). The data appear to be inconsistent with a ($\mu$-hydroxo)diiron(III) site; no resonance enhancement of Fe–($\mu$-OH) stretching modes is expected for such a system, unless coupled to another chromophore (Ling et al., 1992). The only apparent chromophore in the rubrerythrin electronic spectrum likely to approach resonance with 406.7-nm excitation is that at ~365 nm (LeGall et al., 1988), which is most reasonably assigned as a $\mu\text{-}O^{2-} \rightarrow Fe(III)$ charge-transfer transition (Sanders-Loehr et al., 1989).

Finally, no other peaks which shift upon $H_2{}^{18}O$ substitution were detected in the rubrerythrin RR spectrum between 100 and 1700 $cm^{-1}$. This result differs from RR spectra of other ($\mu$-oxo)diiron(III) proteins and synthetic models, which usually show a relatively weak $H_2{}^{18}O$-sensitive peak between 750 and 785 $cm^{-1}$ assigned to $\nu_{as}$(Fe–O–Fe) (Table 2). A weak peak due to $\nu_{as}$(Fe–O–Fe) may be obscured in the RR spectrum of rubrerythrin by the non-$H_2{}^{18}O$ sensitive protein band at 758 $cm^{-1}$ (Figure 2). The $\nu_{as}$(Fe–O–Fe)/$\nu_s$(Fe–O–Fe) intensity ratio, $I_{as}/I_s$, in RR spectra appears to be sensitive to the asymmetry of the Fe–O–Fe coordination sphere (Sanders-Loehr et al., 1989; Gómez-Romero et al., 1989; Norman et al., 1990; Turowski et al., 1990). In the case of synthetic ($\mu$-oxo)diiron(III) complexes, $I_{as}/I_s$ was found to vary from

Table 2: Fe–O–Fe Angles (deg) and Vibrational Frequencies ($cm^{-1}$) of Oxo-Bridged Diiron(III) Clusters in Proteins and Model Complexes[a]

| | | $\nu_s$(FeOFe) | | | $\nu_{as}$(FeOFe) | | |
|---|---|---|---|---|---|---|---|
| | ∠(Fe–O–Fe)[b] | $H_2O$ | $H_2{}^{18}O$ | $\Delta^{18}O$ | $H_2O$ | $H_2{}^{18}O$ | $\Delta^{18}O$ |
| rubrerythrin | 124 | 514[+2][c] | 496[+2] | −18 | nd | | |
| Tribridged Clusters | | | | | | | |
| oxyhemrythrin | 125[d] | 486[+4] | 482 | −14 | 753 | 716 | −37 |
| methemerythrin$N_3^-$ | 128[e] | 507 | 497 | −14 | 768 | 733 | −35 |
| $[Fe_2O(OAc)_2(HBpz_3)_2]$ | 124 | 530 | 513 | −17 | 751 | 718 | −30 |
| $[Fe_2O(OAc)_2(tacn)_2]^{2+}$ | 119 | 540 | 523 | −17 | 749 | 716 | −33 |
| Dibridged Clusters | | | | | | | |
| ribonucleotide reductase | 128[f] | 493[+4] | 480 | −13 | 756 | 721 | −25 |
| $[Fe_2O(OBz)(hdp)_2]^+$ | 129 | 494 | 477 | −17 | 763 | 720 | −43 |
| $[Fe_2O(OBz)(tpa)_2]^{3+}$ | 130 | 497 | 480 | −17 | 772 | 734 | −38 |
| Monobridged Clusters | | | | | | | |
| $[Fe_2O(H_2O)_2(phen)_4]^{4+}$ | 155 | 395 | 390 | −5 | 827 | 786 | −41 |
| $[Fe_2O(hedta)_2]^{2-}$ | 165 | 409 | 407 | −2 | 838 | nd | |

[a] Rubrerythrin data are from this work. Other data are from Sanders-Loehr et al. (1989) and references therein. [b] Rubrerythrin angle calculated as described in the text; all other angles are from X-ray crystal structures. [c] Numbers in square brackets show frequency shifts in deuterated waters. [d] Holmes et al. (1991). [e] Holmes and Stenkamp (1991). [f] Nordlund and Eklund (1993). The other reported angle, 108°, is probably too small for a ($\mu$-oxo)($\mu$-carboxylato) diiron(III) unit.

<0.04 in complexes with identical coordination spheres around each iron to 4.2 in a complex with extremely different coordination spheres around each iron. $I_{as}/I_s$ was found to be 0.2–0.3 for the ($\mu$-oxo)diiron(III) sites in hemerythrin and ribonucleotide reductase, neither of which shows identical coordination spheres for its constituent iron centers (Holmes & Stenkamp, 1991; Holmes et al., 1991; Nordlund & Eklund, 1993). Thus, the inability to observe $\nu_{as}$(Fe–O–Fe) in RR spectra of rubrerythrin might be due to a more symmetrical diiron cluster than is found in either of the former two proteins. A more symmetrical diiron cluster in rubrerythrin than in ribonucleotide reductase has previously been inferred from comparisons of Mössbauer spectra (Ravi et al., 1993). Further studies are in progress to clarify this point and to delineate a function for the unique combination of non-heme iron sites in rubrerythrin.

## ACKNOWLEDGMENT

We thank Dr. Jean LeGall for providing the rubrerythrin samples used in this study and Mr. Ming-Yin Lu for assistance in their purification. We also thank Professors Thomas G. Spiro and Michael K. Johnson for helpful discussions and Drs. Latonya Kilpatrick and Yun-Hua Huang for obtaining some earlier resonance Raman data on *D. vulgaris* rubrerythrin.

## REFERENCES

Czernuszewicz, R. S. (1993) in *Methods in Molecular Biology* (Jones, C., Mulloy, B., & Thomas, A. H., Eds.) Vol. 17, pp 345–374, Humana Press, Totawa, NJ.

Czernuszewicz, R. S., & Johnson, M. K. (1983) *Appl. Spectrosc. 37*, 297–298.

Czernuszewicz, R. S., LeGall, J., Moura, I., & Spiro, T. G. (1986) *Inorg. Chem. 25*, 696–700.

Day M. W., Hsu, B. T., Joshua-Tor, L., Park, J.-B., Zhou, Z. H., Adams, M. W. W., & Rees, D. C. (1992) *Protein Sci. 1*, 1494–1507.

Gómez-Romero, P., Witten, E. H., Reiff, W. M., Backes, G., Sanders-Loehr, J., & Jameson, G. B. (1989) *J. Am. Chem. Soc. 111*, 9039–9047.

Holmes, M. A., & Stenkamp, R. E. (1991) *J. Mol. Biol. 220*, 723–737.

Holmes, M. A., Trong, I. L., Turley, S., Sieker, L. C., & Stenkamp, R. E. (1991) *J. Mol. Biol. 218*, 583–593.

Kurtz, D. M., Jr., & Prickril, B. C. (1991) *Biochem. Biophys. Res. Commun. 181*, 337–341.

LeGall, J., Prickril, B. C., Moura, I., Xavier, A., Moura, J. J. G., & Huynh, B.-H. (1988) *Biochemistry 27*, 1636–1642.

Ling, J., Farooq, A., Karlin, K. D., Loehr, T. M., & Sanders-Loehr, J. (1992) *Inorg. Chem. 31*, 2552–2556.

Nordlund, P., & Eklund, H. (1993) *J. Mol. Biol. 232*, 123–164.

Norman, R. E., Yan, S., Que, L., Jr., Backes, G., Ling, J., Sanders-Loehr, J., Zhang, J. H., & O'Connor, C. J. (1990) *J. Am. Chem. Soc. 112*, 1554–1562.

Pierik, A. J., Wolbert, R. B. G., Portier, G. L., Verhagen, M. F. J. M., & Hagen, W. R. (1993) *Eur. J. Biochem. 212*, 237–245.

Ravi, N., Prickril, B. C., Kurtz, D. M., Jr., & Huynh, B.-H. (1993) *Biochemistry 33*, 8487–8491.

Sanders-Loehr, J. (1989) in *Iron Carriers and Iron Proteins* (Loehr, T. M., Ed.) pp 373–466, VCH Press, New York.

Sanders-Loehr, J., Wheeler, W. D., Shiemke, A. K., Averill, B. A., & Loehr, T. M. (1989) *J. Am. Chem. Soc. 111*, 8084–8093.

Sieker, L. C., Turley, S., Prickril, B. C., & LeGall, J. (1988) *Proteins 3*, 184–186.

Spiro, T. G., Czernuszewicz, R. S., & Han, S. (1988) in *Biological Applications of Raman Spectroscopy* (Spiro, T. G., Ed.) Vol. 3, pp 523–554, Wiley-Interscience, New York .

Stenkamp, R. E., Holmes, M., Sieker, L. C., Trong, I. L., Turley, S., & LeGall, J. (1992) American Crystallographic Association, Abstr. 20, 140.

Turowski, P. N., Armstrong, W. H., Roth, M. E., & Lippard, S. J. (1990) *J. Am. Chem. Soc. 112*, 681–690.

Yachandra, V. K., Hare, J., Moura, I., & Spiro, T. G. (1983) *J. Am. Chem. Soc. 105*, 6455–6461.

Wilkins, R. G. (1992) *Chem. Soc. Rev. 21*, 171–178.

Wing, R. M., & Callahan, K. P. (1969) *Inorg. Chem. 8*, 871–874.